

Observation of frequency modulation in second-harmonic generation of ultrashort pulses

H. J. Bakker, W. Joosen, and L. D. Noordam

FOM—Institute for Atomic and Molecular Physics, Kruislaan 407, 1098 SJ Amsterdam, The Netherlands

(Received 15 July 1991)

We study both experimentally and theoretically the intensity and frequency profile of the pulse that is generated by second-harmonic generation with phase mismatch of a pulse with a duration of 50 fs. Experimentally, we determine the shape and the frequency of the generated pulse by correlating it with a second fundamental pulse and by measuring the spectra of the generated pulse. Theoretically, we solve numerically the coupled differential equations that describe the nonlinear interaction. We show that for ultrashort pulses the effects of phase mismatch, depletion, and group-velocity differences between the fundamental and the second harmonic strongly influence the intensity profile and the frequency spectrum of the second-harmonic pulse. We find that in second-harmonic generation with phase mismatch the frequency of the generated pulse becomes modulated.

PACS number(s): 42.65.Ky, 42.65.Re

I. INTRODUCTION

Ever since the first observation of second-harmonic generation (SHG) in 1961 [1], this second-order nonlinear optical process has been extensively studied. Both improvement of the efficiency and understanding of the fundamental aspects of the process have been the subject of many studies [2,3]. For SHG of ultrashort pulses it turns out to be very difficult to get both a large conversion efficiency and to avoid distortion of the generated second-harmonic-pulse shape. It is important to know how the time profile and the frequency spectrum of the pulses generated via SHG of ultrashort pulses change if these pulses are to be applied in spectroscopic studies. It was shown that for ultrashort pulses the effects of a group-velocity difference between the fundamental and the second harmonic become important and that this can lead to very interesting phenomena in the intensity profile of the generated second-harmonic pulse [4–6]. A large group-velocity difference will lead to a lengthening of the generated second-harmonic pulse [4]. The pulse shape of the second harmonic will become essentially square if there is no depletion in the phase-matched SHG process and the difference in travel time through the nonlinear crystal is much longer than the pulse duration of the fundamental. This was experimentally observed in SHG of picosecond-long pulses in LiNbO_3 crystals of different lengths [5] and in SHG of femtosecond pulses in a long potassium dihydrogen phosphate (KDP) crystal [6].

If the SHG process takes place with a phase mismatch, there will be destructive interference effects in the generation of the second-harmonic-pulse shape. This effect was studied both analytically [7,8] and, in combination with depletion, numerically [9,10], and it was found that phase mismatch in combination with a large difference in group velocity leads to a two-peak structure for the second-harmonic-pulse shape. This structure is the result of the fact that the second-harmonic light generated in the front

part of the fundamental pulse travels along the fundamental pulse and destructively interferes with the second-harmonic light generated in the rear part, so that the net energy conversion will be very small. This destructive interference does not occur for light generated in the rear wing of the fundamental pulse at the beginning and in the front wing at the end of the nonlinear material. The final pulse structure will thus mainly consist of two peaks that are separated by the difference in time that the fundamental and the second harmonic need to travel through the crystal.

In a recent study, we observed this two-peak pulse shape, and we compared the experimental results with numerical calculations [6]. It was demonstrated that phase modulation of the fundamental pulse influences the destructive interference and the pulse shape of the second harmonic.

When, apart from SHG, third-order nonlinear optical processes are important, it was shown that the generated second harmonic acquires a very complicated multippeak structure [11,12]. This structure is the result of the phase modulation caused by the third-order processes self-phase-modulation (SPM) and induced phase modulation (IPM) coupled with the interference effects in the SHG process.

In this paper we present experimental results on the amplitude and frequency structure of the pulse shape that is generated via SHG of femtosecond pulses in a long KDP crystal. For KDP the effects of third-order nonlinear optical processes can be neglected [16]. We determine the intensity profile of the second-harmonic pulse by correlating it with the fundamental pulse in a second short KDP crystal. We find experimental evidence that the frequency of the second-harmonic pulse is modulated. This frequency modulation is due to the combined effects of phase mismatch and differences in group velocity in SHG and is not the result of third-order nonlinear optical processes. We compare the experimental results with nu-

merical calculations based on the theory of Ref. [10].

This paper is organized as follows. In Sec. II the experimental setup is described. Section III contains a theoretical description of the SHG process and the difference-frequency generation process that is used in the cross correlation of the second-harmonic-pulse shape with the fundamental. In Sec. IV the method of numerical evaluation of the equations of the theoretical section is described. In Sec. V experimental results are presented, and these results are compared with the numerical calculations.

II. EXPERIMENT

The experimental setup is schematically depicted in Fig. 1. As a light source for the experiments we used a high-power femtosecond-type dye-laser system [13]. The oscillator is a colliding-pulse mode-locked (CPM) laser, which is amplified in a four-stage dye amplifier. The dye amplifier consists of four side-pumped bethune-type [14] dye cells. In the first cell we use as dye kiton red, dissolved in a mixture of water (98.5 vol %) and ammonyx LO (1.5 vol %). In the following three cells we use sulforhodamine 640 dye, dissolved in methanol. The dye is pumped at a repetition rate of 10 Hz by the frequency-doubled output of a Q -switched injection-seeded neodymium-doped yttrium aluminum garnet (Nd:YAG) laser. The amplified spontaneous emission (ASE) is suppressed by spatial filtering between the cells and a saturable absorber after the third dye cell. In this way pulses of about $200 \mu\text{J}$ are generated. The amplified CPM pulses are sent into a folded four-prism compressor, that compensates for frequency chirp due to the amplifier. The pulse duration is measured to be 50 fs with a standard autocorrelation setup. The spectrum of these pulses is centered around 615 nm, and the width of the spectrum is 10 nm (260 cm^{-1}).

Part of the amplified CPM pulse ($20 \mu\text{J}$) is divided by a

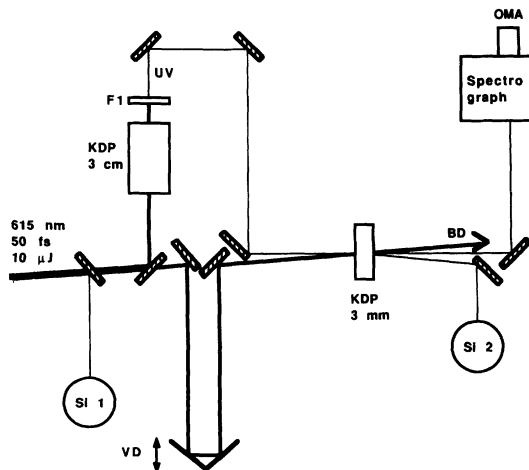


FIG. 1. Experimental setup used for analyzing the uv-pulse shapes that are generated via SHG in a 3-cm KDP crystal. VD, variable delay; F1, short-pass filter; Si 1, Si 2, photodiodes; BD, beam dump; OMA, optical multichannel analyzer.

beam splitter into two pulses, one of which is doubled (type I: $o+o \rightarrow e$) in a KDP crystal of 3-cm length. The frequency contents of the generated second harmonic is measured by a monochromator (SPEX 1870) in combination with an optical multichannel analyzer (OMA).

The time profile of the generated second-harmonic pulses is determined in a cross correlation setup, in which the second-harmonic-pulse shape is correlated with the second part of the amplified CPM pulse [15]. The shape of the second harmonic cannot be measured via sum-frequency generation since nonlinear crystals are generally not transparent at 205 nm. Therefore we generated the difference frequency of the uv and the fundamental in a 3-mm KDP crystal. In this process a second beam at approximately 615 nm comes out of the mixing crystal (type I: $e-o \rightarrow o$). In a noncollinear setup this second beam is angularly displaced and can be measured background free. By measuring the amount of generated energy at the difference frequency as a function of the delay between uv and second fundamental pulse, the cross correlation function of the second-harmonic-pulse shape with the amplified CPM pulse is determined. The experiments are computer controlled. A typical experiment consists of six scans of the variable delay over $1380 \mu\text{m}$. Each scan consists of 70 points of delay. At each point of delay the difference-frequency signal and the input signal of 20 laser shots are stored.

III. THEORY

The description of the second-order nonlinear interaction between three classical electromagnetic fields can be greatly simplified if a few assumptions are used. In the first place, only the interaction due to the electrical component of the fields is considered. Second, the transverse variation of the fields is neglected. Under these assumptions the electric component \mathcal{E}_i ($i=1,2,3$) of the three fields propagating collinearly along the z axis can be written as a product of an electric-field amplitude and a plane wave

$$\mathcal{E}_i(z,t) = E_i(z,t) \exp[i(k_i z - \omega_i t)], \quad (1)$$

with E_i the complex amplitude, k_i the wave vector, and ω_i the central angular frequency of field \mathcal{E}_i .

The interaction results in an energy transfer between the fields. Therefore, the field amplitudes are expected to change while they propagate through the nonlinear material. This change in amplitude can be described by three coupled differential equations. These equations are derived from Maxwell's equations and can be simplified to first-order differential equations if the slowly varying amplitude approximation is used. This approximation is valid if the change in amplitude of the fields is significant only after the fields traveled over a distance much longer than their wavelength. When the standard equations that describe the nonlinear interaction are transformed, we obtain the following set of equations [10]:

$$\frac{\partial}{\partial z} E_1 = \frac{i\omega_1 \chi_{\text{eff}}^{(2)}}{2n_1 c} E_2^* E_3, \quad (2)$$

$$\left[\frac{\partial}{\partial z} + \left(\frac{1}{v_2^\xi} - \frac{1}{v_1^\xi} \right) \frac{\partial}{\partial \eta} \right] E_2 = \frac{i\omega_2 \chi_{\text{eff}}^{(2)}}{2n_2 c} E_1^* E_3, \quad (3)$$

$$\left[\frac{\partial}{\partial z} + \left(\frac{1}{v_3^\xi} - \frac{1}{v_1^\xi} \right) \frac{\partial}{\partial \eta} \right] E_3 = \frac{i\omega_3 \chi_{\text{eff}}^{(2)}}{2n_2 c} E_1 E_2 + i\Delta k E_3, \quad (4)$$

with E_i the complex amplitude of the electric field, z the distance in the crystal, v_i^ξ the group velocity of field i , n_i the refractive index of field i , η the transformed time ($\eta = t - z/v_1^\xi$), $\chi_{\text{eff}}^{(2)}$ the effective second-order susceptibility, and Δk the phase mismatch. The value of $\chi_{\text{eff}}^{(2)}$ is determined by the directions of polarization of the fields and the elements of the second-rank tensor $\chi^{(2)}$.

In the case of SHG the fields E_1 and E_2 become indistinguishable so that these two separate fields can be replaced by one fundamental field. However, the nonlinear coupling term that changes this fundamental field becomes twice as large because generation of one photon at ω_3 now costs two photons of the fundamental field instead of one photon at ω_1 and one photon at ω_2 . The two coupled equations (2) and (3) now reduce to one equation for the fundamental field with the coupling term multiplied by two.

When the field E_3 is generated, the phase evolution of this field is determined by both the interaction and the phase mismatch. When the field E_3 loses overlap with the field E_1 , due to the difference in group velocity, the phase evolution of E_3 is solely determined by the phase mismatch. In that case the phase difference between E_3 and E_1 accumulates with Δkz . Therefore the phase of the complex amplitude will monotonically increase or decrease over the second-harmonic-pulse shape depending on the sign of Δk . The light generated in the beginning of the nonlinear material will have the highest accumulated phase difference. An increase or decrease of the phase of the complex amplitude over the pulse implies a change of the central frequency

$$\Delta\nu = - \frac{\Delta\phi}{2\pi\Delta t}. \quad (5)$$

This change in frequency depends on the value of Δk for SHG of the central frequency of the fundamental pulse and the difference in group velocity between the two pulses and is equal to

$$\Delta\nu = - \frac{\Delta k}{2\pi(1/v_3^\xi - 1/v_1^\xi)}. \quad (6)$$

The frequency of the light of the second-harmonic-pulse shape differs from the doubled central frequency of the fundamental pulse. In the Appendix it is shown that this shifted frequency is exactly the frequency for which the SHG process is phase matched.

With a second crystal the amplitude and frequency structure of the generated pulse can be analyzed. In this second crystal the difference frequency of the second harmonic and the fundamental can be generated, and the energy of this light can be monitored as a function of the delay between the two pulses and the angle of the second

crystal. If we assume that the second-harmonic pulse is not locally depleted in this process and that the differences in group velocity are negligible in this second crystal, the third of the three equations can be easily solved: $E_3(z) = E_3(0)e^{i\Delta kz}$. If we also assume that the fundamental pulse (E_2) is not significantly amplified and the solution for E_3 is substituted in the equation for the difference frequency (E_1), this equation can easily be solved. If we multiply this solution with its complex conjugate we get the following expression for $|E_1|^2$, which is proportional to the intensity

$$|E_1(z, \eta)|^2 = \frac{\omega_1^2 (\chi_{\text{eff}}^{(2)})^2}{4n_1^2 c^2} \frac{\sin^2(\frac{1}{2}\Delta kz)}{(\frac{1}{2}\Delta kz)^2} |E_2(0)|^2 |E_3(0, \eta)|^2. \quad (7)$$

Due to the $\sin^2(\frac{1}{2}\Delta kz)/(\frac{1}{2}\Delta kz)^2$ function, the efficiency of the difference-frequency generation oscillates as a function of Δk and thus as a function of the angle of the second crystal. The sensitivity of the conversion efficiency for Δk makes it possible to determine the time-profile of the second-harmonic pulse as a function of the frequency.

IV. NUMERICAL EVALUATION

As described previously, the experiment consists of two subsequent nonlinear optical processes. For each nonlinear optical process we use a different numerical approach to simulate the experimental correlation traces. We integrate the two coupled differential equations describing the SHG process with a Runge-Kutta method that has fourth-order accuracy in both time and distance [9]. In this method the effects of depletion of the fields, differences in group velocity, and phase mismatch are incorporated. The effect of group-velocity dispersion within the bandwidth of the pulses is not taken into account. The time profile of the pulses is defined in a grid of 500 time points, and the pulses that come out of the crystal are calculated by integrating the equations with steps of 0.02 mm. As a pulse shape for the fundamental pulse we used a Gaussian shape with a width of 50 fs.

The second-harmonic-pulse shape that is calculated with this first program is used as input for a second program. In this second program the difference-frequency mixing with a second fundamental Gaussian pulse of 50 fs is simulated. It is assumed that in this process neither the amplitude of the second-harmonic pulse nor the amplitude of the fundamental pulse changes. Due to the difference in group velocity between the fundamental and the second harmonic, the difference-frequency light that has approximately the fundamental frequency travels together with the strong fundamental pulse along a part of the second-harmonic pulse shape. In each time point of this part of the second harmonic, the amplitude, the local frequency, and the Δk for difference-frequency generation are evaluated. With this information the electric field of the generated difference frequency can be calculated for each time point, and these fields are summed with the proper phase. In this way the effects of group-velocity differences and variation of Δk within the bandwidth of the second-harmonic pulse are incorporated.

V. RESULTS AND DISCUSSION

We performed experiments for two different intensities of the fundamental 615-nm pulse in order to investigate the effects of depletion. In addition, we used two different signs of phase mismatch, in order to investigate the influence of the sign of the phase mismatch on the frequency spectrum of the generated second harmonic. If the fundamental pulse is not phase modulated (not chirped), the intensity profile of the second-harmonic-pulse shape is not influenced by this sign, because in this case the destructive interference effects in the SHG pro-

cess only depend on the magnitude of Δk . At the lowest intensity of 4.5 GW/cm^2 , $\Delta k = 50.7 \text{ cm}^{-1}$ and at the highest intensity of 13.5 GW/cm^2 , $\Delta k = -50.4 \text{ cm}^{-1}$. The experimental results are compared with numerical calculations.

In Figs. 2 and 3 we present calculated electric-field amplitude, phase and intensity profiles of the uv pulse that can be generated in a 3-cm KDP crystal. We present the real and imaginary part of the amplitude of the electric field assuming that the central wavelength of the electric field is equal to 307.5 nm. We see that the phase of the electric-field amplitude strongly changes over the uv

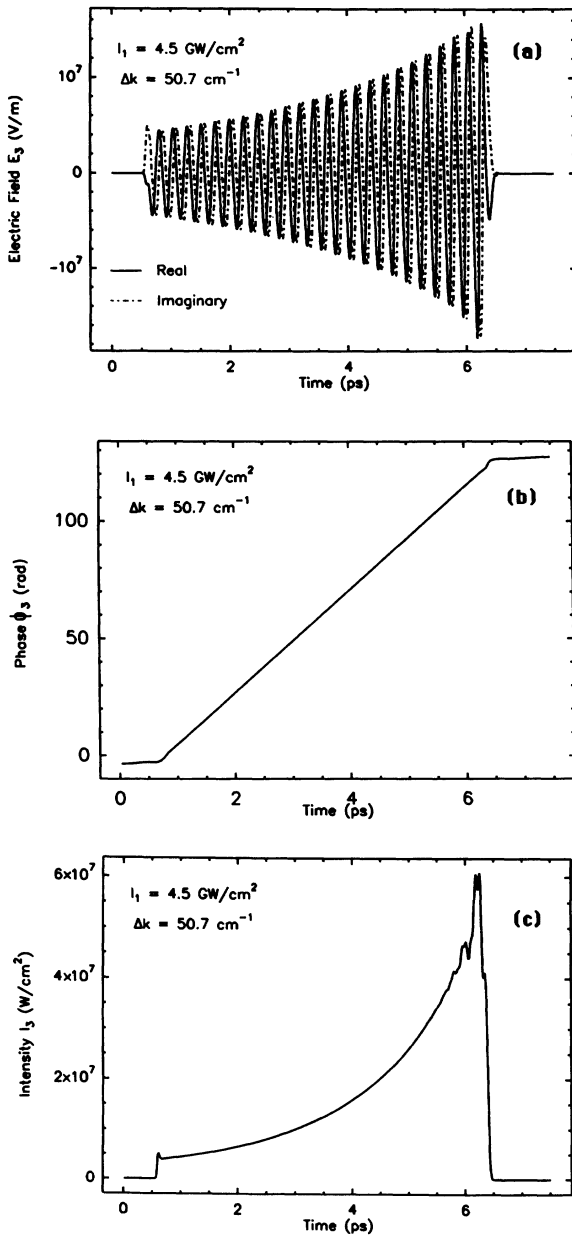


FIG. 2. Numerically calculated electric-field amplitude (a), phase (b), and intensity profile (c) of the uv pulse that can be generated via SHG with phase mismatch of a 615-nm pulse with a pulse duration of 50 fs in a 3-cm KDP crystal.

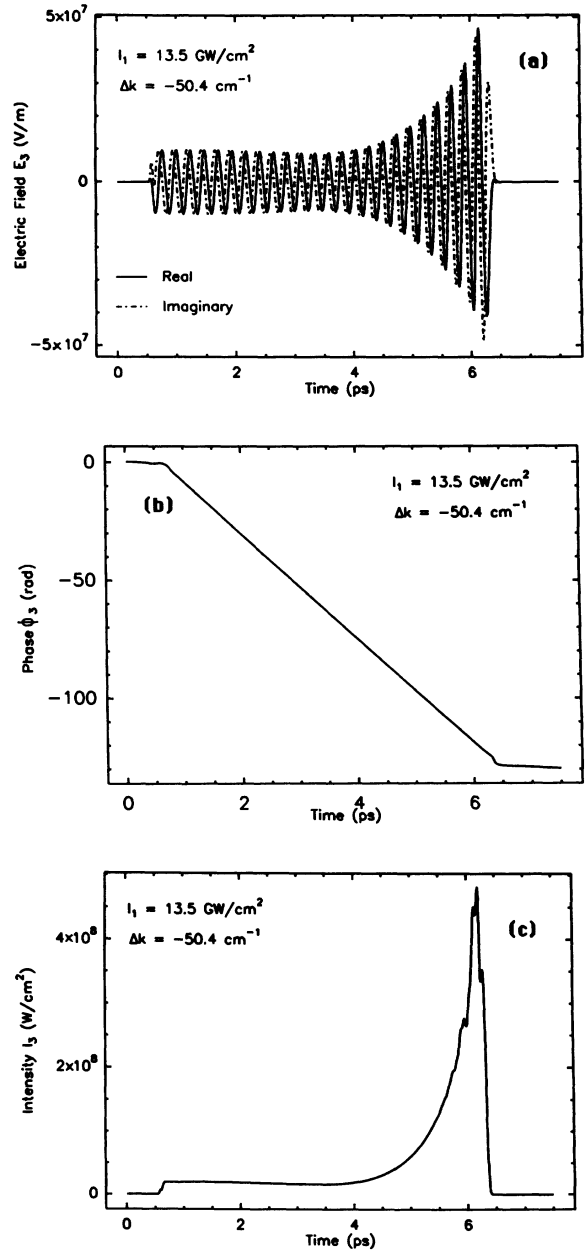


FIG. 3. As in Fig. 2, but for a different intensity of the fundamental pulse and with a different phase mismatch in the SHG process.

pulse as a result of the phase mismatch. In case of a positive Δk [Fig. 2(b)] we observe a linear increase of the phase over the pulse, whereas in the case of a negative Δk we observe a linear decrease [Fig. 3(b)].

The intensity profiles [Figs. 2(c) and 3(c)] clearly show the effects of depletion. The intense right part of the pulse is generated by a still undepleted fundamental pulse in the beginning of the KDP crystal, and the weak left part of the pulse is generated by a strongly depleted fundamental pulse at the end of the crystal. This weak part comes out of the crystal first. We do not observe an uv-pulse structure consisting of two peaks separated by the difference in travel time between uv and fundamental light through the KDP crystal. This is due to the fact that the fundamental pulse is very short. In the time domain we can understand this as follows. For a fundamental pulse of 50 fs, the interaction length in the crystal during which the uv light travels along the fundamental pulse is that short that the uv light generated in the front wing has not yet acquired the opposite phase when it overlaps with the rear wing of the fundamental pulse. Therefore only a small part of the generated uv light will be reconverted. We can also understand this phenomenon in the frequency domain. As a result of the short pulse duration of the fundamental pulse, the band-

width will be large. Therefore half the shifted frequency of the uv pulse is still well within the bandwidth of the fundamental pulse, which implies that the shifted uv frequency can efficiently be generated. If the phase mismatch or the pulse duration had been larger, the uv pulse would obtain a two-peak pulse shape.

In Figs. 4 and 5 we present the experimental and theoretical spectra of the generated uv pulse. We observe that the spectra are narrow and are shifted with respect to the second harmonic of the central fundamental wavelength of 615 nm. For positive Δk the phase increases over the uv pulse, which implies a shift of 1.35 nm of the wavelength to a higher value [Eq. (5)]. For negative Δk , the phase decreases over the uv pulse, which corresponds to a shift of the wavelength of 1.35 nm to a lower value. In Fig. 5 we show the same spectra, but the vertical scale has been expanded by a factor of 100. We observe that both uv spectra have a stronger tail towards 307.5 nm than away from 307.5 nm.

The uv spectra are not symmetric, which indicates that the phase increase is not purely linear over the whole uv-pulse shape. In case the phase increase had been linear, the pulse could have been described as a pulse with a shifted central frequency without phase modulation. The spectrum of such a pulse is only determined by the amplitude profile and is therefore completely symmetric. In that case all the time points of the pulse have the same

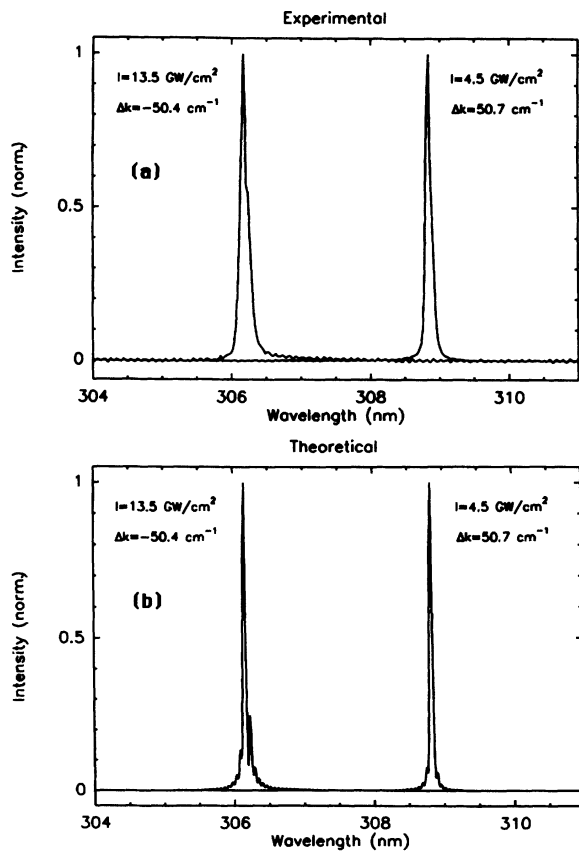


FIG. 4. (a) Experimental and (b) theoretical spectra of uv pulses generated via SHG with phase mismatch of a 615-nm pulse with a pulse duration of 50-fs in a 3-cm KDP crystal for two intensities and two values of phase mismatch.

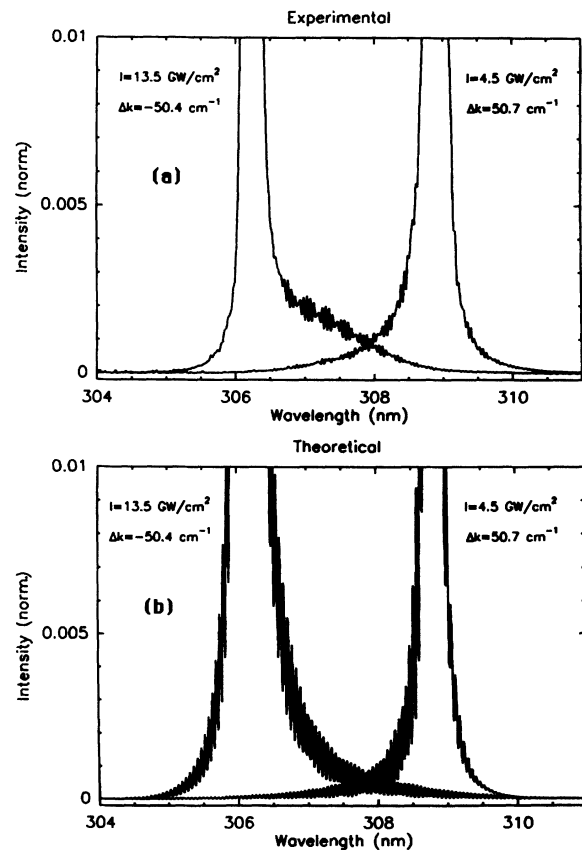


FIG. 5. As in Fig. 4 but with the vertical scale expanded by a factor of 100.

frequency contents, which implies that the frequency of the pulse is not modulated. In Figs. 2(b) and 3(b) it can be seen that the phase dependence on time is not purely linear but changes from horizontal in the wings to linear increasing or decreasing in the central part of the pulse. This implies that going from the outermost parts of the wings to the beginning of the central part the wavelength changes from 307.5 to 308.85 nm [Fig. 2(b)] or to 306.15 nm [Fig. 3(b)].

We observe that the spectrum of the uv pulse becomes broader with increasing intensity of the fundamental pulse. This is due to the fact that at higher intensities of the fundamental the depletion effect is stronger, so that the intense part of the resulting uv pulse covers a smaller time interval. This leads to a broadening of the spectrum.

Both the experimental and the theoretical spectra exhibit rapid oscillations of the amplitude of the frequency components. These fringes in the spectrum are due to the very steep wings of the uv pulse. These steep wings mean that the Fourier transform has $\sin^2(x)/x^2$ functional form. We observe these fringes every 5.5 cm^{-1} , which corresponds with a time interval of 6 ps. This time interval is approximately the duration of the uv-pulse shape. In the experimental spectrum the fringes are less

well resolved due to the limited resolution of the spectrograph and the OMA.

In order to investigate the time profile of the generated uv pulses, we correlate the pulses with a second fundamental pulse in a 3-mm KDP crystal. In Figs. 6 and 7 we present experimental and calculated cross correlation traces for four different uv wavelengths for which the difference-frequency generation in the 3-mm KDP crystal is phase matched. In all cases the calculated result represented by the solid line is in good agreement with the experimental result. We observe that the generated energy in the difference-frequency generation process is at its highest value when the phase-matched wavelength in the 3-mm KDP crystal exactly equals the shifted wavelength that was generated in the 3-cm KDP crystal. In Figs. 6(a) and 7(a) we observe that the cross correlation traces strongly resemble the calculated intensity profiles of the uv pulses [Figs. 2(c) and 3(c)].

In case the uv pulse does not deplete, the difference-frequency generation process can be described with Eq. (7). The efficiency of this process is proportional to $\sin^2(\frac{1}{2}\Delta kl)/(\frac{1}{2}\Delta kl)^2$ with l the interaction length in the 3-mm KDP crystal. When the phase-matched wavelength is changed in such a way that for the shifted wavelength $\Delta kl = \pm 2\pi$, the efficiency becomes equal to zero.

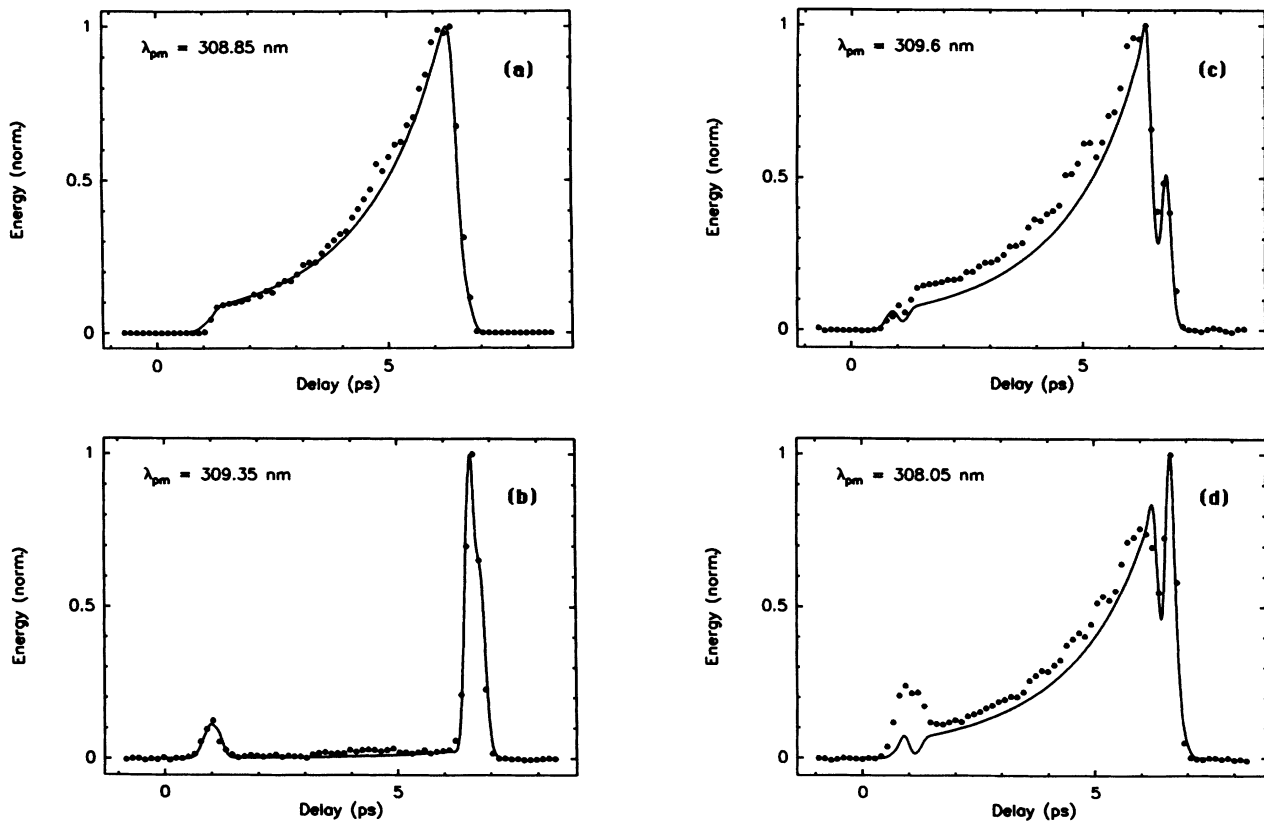


FIG. 6. Experimental and theoretical cross correlation traces resulting from correlating a uv-pulse shape with a 615-nm pulse with a pulse duration of 50 fs in a 3-mm KDP crystal. The uv-pulse shape is generated by SHG with $\Delta k = 50.7 \text{ cm}^{-1}$ of a 615-nm pulse with a pulse duration of 50 fs and a maximum intensity of 4.5 GW/cm^2 . The four correlation traces represent four different uv wavelengths for which the difference-frequency generation process in the 3-mm crystal is phase matched.

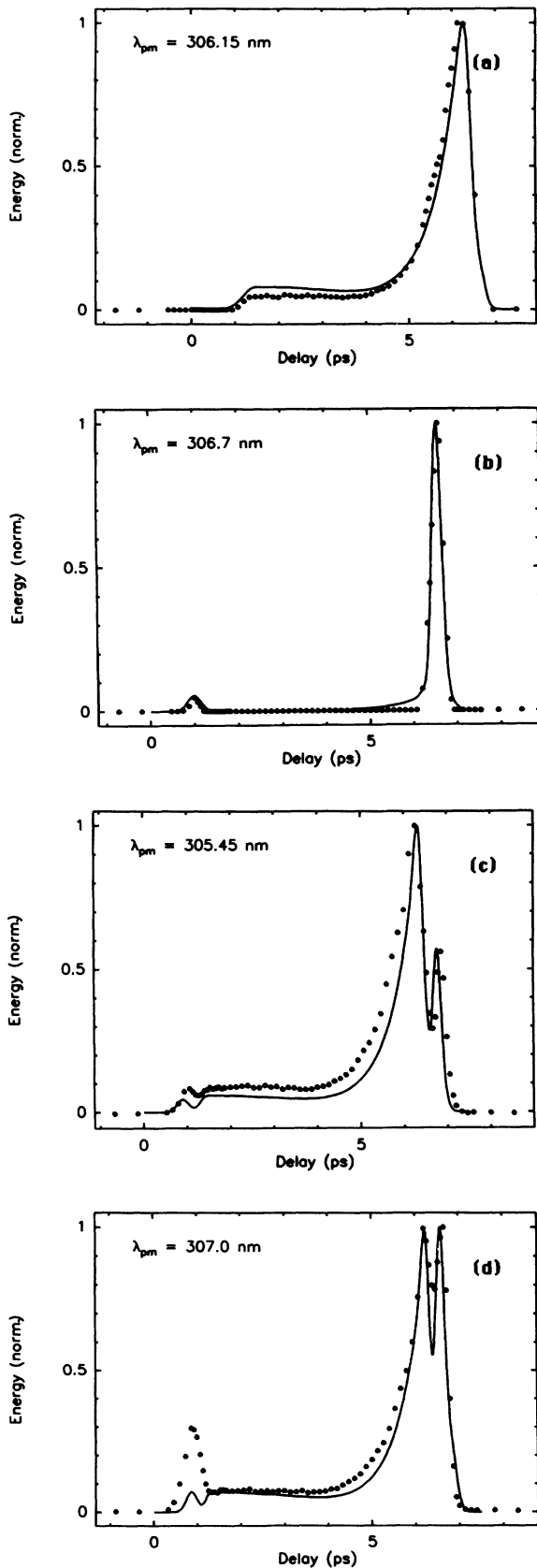


FIG. 7. As in Fig. 6, but for a uv-pulse shape generated by SHG with $\Delta k = -50.4 \text{ cm}^{-1}$ of a 615-nm pulse with a pulse duration of 50 fs and a maximum intensity of 13.5 GW/cm^2 .

In that case we observe that the cross correlation trace consists of two peaks [Fig. 6(b) and 7(b)] which correspond in time with the wings of the uv pulse. These peaks can be the result of the fact that the frequency contents of the wings is somewhat different from that of the central part of the uv pulse. However there is one other important effect that makes the efficiency in the wings different from zero. As a result of the group-velocity differences between the uv light and the fundamental light, the travel time through the 3-mm KDP crystal of the fundamental pulse will be 600 fs shorter than the travel time of the uv pulse. Therefore the fundamental pulse does not necessarily overlap with the uv pulse over the whole length of the KDP crystal. For instance, if the fundamental pulse enters the crystal 400 fs after the front wing of the uv pulse, it will only have significant interaction with the uv pulse in the first 2 mm of the KDP crystal. If the fundamental pulse enters the KDP crystal 400 fs after the rear wing of the uv pulse, then it will only have significant interaction in the last mm of the KDP crystal. Therefore the magnitude of the effective Δkl will be smaller than 2π in the wings of the uv pulse, so that the efficiency of the difference-frequency generation process will be different from zero.

When the phase-matched wavelength is changed in such a wave that $\Delta kl = \pm 3\pi$ for the central part of the uv pulse [Figs. 6(c), 6(d), 7(c), and 7(d)] the $\sin^2(\frac{1}{2}\Delta kl)/(\frac{1}{2}\Delta kl)^2$ function has its second maximum. In this case we observe a significant central part in the cross correlation trace. We also observe again the two peaks in the wings, and we observe dips in the efficiency of difference-frequency generation between the peaks and the central part. The delays of the fundamental pulse for which we observe a dip in the efficiency are those for which the effective interaction length is approximately 2 mm, so that for these delays the effective value of Δkl is equal to $\pm 2\pi$. The two peaks can again be the result of the fact that the effective Δkl in the wings will be smaller than 2π .

We observe that both in the experimental cross correlation trace and in the numerical simulation the two peaks are stronger compared to the central part of the cross correlation in Figs. 6(d) and 7(d) than in Figs. 6(c) and 7(c). This difference in intensity cannot be explained from the dependence of the conversion efficiency on Δk and the interaction length because the $\sin^2(\frac{1}{2}\Delta kl)/(\frac{1}{2}\Delta kl)^2$ function is symmetric in Δkl . With the measurement of the spectrum we already found that in case the SHG process takes place with a phase mismatch, the spectrum is broadened towards 307.5 nm. Therefore we explain the difference in intensity of the peaks from the fact that in Figs. 6(d) and 7(d) the phase-matched wavelength is much closer to the central wavelength of 307.5 nm than in Figs. 6(c) and 7(c). This implies that the frequency modulation of the uv pulse is such that the wavelength in the wings of the uv-pulse shape is closer to 307.5 nm than the wavelength of the central part of the uv-pulse shape. This experimental observation agrees very well with the calculated phase dependence on time in the phase profiles of Figs. 2(b) and 3(b).

The difference in the dependence of the phase on time between the wings and the central part of the pulse can

be understood in the following way. The time points in the uv-pulse shape all correspond with distances in the nonlinear material at which the light was most efficiently generated. In the central part of the pulse the linear increase (positive Δk) or decrease (negative Δk) of the phase of the complex electric-field amplitude over the time profile corresponds with a linear decrease of the distance at which the uv light was most efficiently generated by the maximum of the fundamental pulse. In the outer parts of the wings however, the distance at which the light was most efficiently generated is for all time points the same. For the rear wing this distance corresponds with the beginning of the crystal, and for the front wing this distance corresponds with the end of the crystal. Therefore all time points in the outer parts of the wings have the same accumulated phase of the complex electric-field amplitude so that in these parts of the time profile of the second-harmonic pulse this phase does not increase or decrease.

The second-harmonic-pulse shapes that we can generate with a long crystal have special properties that make them interesting for spectroscopic applications. The frequency spectrum of these pulses is very narrow because of the well-defined frequency of the long part of the pulse in between the wings. The central frequency of the pulses can be tuned by changing the phase mismatch. This tuning by changing the phase mismatch for the central frequency hardly changes the conversion efficiency because the frequency spectrum of the fundamental is very broad. In spite of their narrow frequency spectrum these pulses have still very steep wings with a rise time that corresponds with the very short pulse duration of the fundamental. Therefore in spite of their length, these pulses still offer a very good time resolution. They may especially be useful in the time-resolved study of the relaxation excitations that take place on a time scale between the overall duration of the second-harmonic pulse and the rise time of the wings. These excitations can be pumped very efficiently because the narrow spectrum of the pulse will be mostly in the absorption band, and they can still be studied with a time resolution that is comparable with the pulse duration of the fundamental. Another possible application for these pulses may be in experiments in which a short switch-on time of the light is of vital importance.

VI. CONCLUSIONS

When an ultrashort pulse is frequency doubled in a long dispersive crystal, the resulting pulse will be stretched and the spectrum of this pulse will be narrow.

If the process takes place with a phase mismatch, the intensity profile will be influenced by destructive interference effects, and the spectrum will shift away from the second harmonic of the frequency of the fundamental pulse. The spectrum becomes asymmetric and is broadened towards the second harmonic of the central fundamental wavelength. This indicates that the frequency of the second-harmonic-pulse shape is modulated.

The second-harmonic-pulse shape can be determined by correlating the pulse with a second part of the funda-

mental pulse in a short second crystal. From these time-resolved measurements it follows that the frequencies in the wings of the second-harmonic-pulse shape are closer to the second harmonic of the central fundamental frequency than the frequency of the central part of the uv-pulse shape. The experimental results agree very well with numerical calculations in which the SHG and the cross correlation processes are simulated.

Finally, the special properties of the pulses that are generated via SHG of ultrashort pulses in a long crystal make them very useful for certain time-resolved spectroscopic applications.

ACKNOWLEDGMENTS

The authors wish to acknowledge very useful discussions with Ad Lagendijk. The work in this paper is part of the research program of the "Stichting voor Fundamenteel Onderzoek van de Materie" (Foundation for Fundamental Research on Matter) and was made possible by financial support from the "Nederlandse Organisatie voor Wetenschappelijk Onderzoek" (Netherlands Organization for the Advancement of Research).

APPENDIX

In this appendix we show that the shifted frequency that results from the equation for Δv [Eq. (6)] is exactly the frequency for which $\Delta k = 0$ in SHG. For the group velocity v_i^g we use the following equation:

$$v_i^g = \frac{c}{n_{i,0} + v_{i,0} \delta n / \delta v |_{v=v_{i,0}}}, \quad (\text{A1})$$

with $v_{i,0}$ the central frequency of field i . If we substitute this in Eq. (6) we find for Δk

$$\Delta k(2\nu_{1,0} \rightarrow \nu_{3,0}) = \frac{2\pi \Delta v}{c} \left[\nu_{1,0} \frac{\delta n}{\delta v} \Big|_{v=\nu_{1,0}} + n_{1,0} - \nu_{3,0} \frac{\delta n}{\delta v} \Big|_{v=\nu_{3,0}} - n_{3,0} \right]. \quad (\text{A2})$$

For Δk we use the following equation:

$$\Delta k(2\nu_{1,0} \rightarrow \nu_{3,0}) = 2\nu_{1,0}(n_{3,0} - n_{1,0}) \frac{2\pi}{c}. \quad (\text{A3})$$

Substitution leads to

$$\frac{2\pi}{c} \left[\nu_{3,0} n_{3,0} + \Delta v \nu_{3,0} \frac{\delta n}{\delta v} \Big|_{v=\nu_{3,0}} + n_{3,0} - 2\nu_{1,0} n_{1,0} - \Delta v \nu_{1,0} \frac{\delta n}{\delta v} \Big|_{v=\nu_{1,0}} - n_{1,0} \right] = 0. \quad (\text{A4})$$

If terms in Δv^2 can be neglected, this equation can be written as

$$\frac{2\pi}{c} \left[(\nu_{3,0} + \Delta\nu) \left[n_{3,0} + \Delta\nu \frac{\delta n}{\delta\nu} \Big|_{\nu=\nu_{3,0}} \right] - (2\nu_{1,0} + \Delta\nu) \left[n_{1,0} + \frac{1}{2}\Delta\nu \frac{\delta n}{\delta\nu} \Big|_{\nu=\nu_{1,0}} \right] \right] = 0. \quad (\text{A5})$$

If we define the shifted frequencies ν_3 and ν_1 as $\nu_3 = \nu_{3,0} + \Delta\nu$ and $\nu_1 = \nu_{1,0} + \frac{1}{2}\Delta\nu$, it follows that

$$\frac{2\pi}{c} (\nu_3 n_3 - 2\nu_1 n_1) = 0 = \Delta k (2\nu_1 \rightarrow \nu_3). \quad (\text{A6})$$

-
- [1] P. A. Franken, A. E. Hill, C. W. Peters, and G. Weinreich, *Phys. Rev. Lett.* **7**, 118 (1961).
 [2] R. C. Eckardt and J. Reintjes, *IEEE J. Quantum Electron.* **QE-20**, 1178 (1984).
 [3] R. D. Kuhlke and U. Herpers, *Opt. Commun.* **69**, 75 (1988).
 [4] J. Comly and E. Garmire, *Appl. Phys. Lett.* **12**, 7 (1968).
 [5] S. L. Shapiro, *Appl. Phys. Lett.* **13**, 19 (1968).
 [6] L. D. Noordam, H. J. Bakker, M. P. de Boer, and H. B. van Linden van den Heuvell, *Opt. Lett.* **15**, 1464 (1990).
 [7] J. T. Manassah and O. R. Cockings, *Opt. Lett.* **12**, 1005 (1987).
 [8] J. T. Manassah, *Appl. Opt.* **27**, 4365 (1988).
 [9] H. J. Bakker, P. C. M. Planken, and H. G. Muller, *J. Opt. Soc. Am. B* **6**, 1665 (1989).
 [10] H. J. Bakker, P. C. M. Planken, L. Kuipers, and A. Lagendijk, *Phys. Rev. A* **42**, 4085 (1990).
 [11] P. P. Ho, Q. Z. Wang, D. Ji, and R. R. Alfano, *Appl. Phys. Lett.* **54**, 111 (1989).
 [12] P. P. Ho, D. Ji, Q. Z. Wang, and R. R. Alfano, *J. Opt. Soc. Am. B* **7**, 276 (1990).
 [13] L. D. Noordam, W. Joosen, B. Broers, A. ten Wolde, A. Lagendijk, H. B. van Linden van den Heuvell, and H. G. Muller, *Opt. Commun.* **85**, 331 (1991).
 [14] D. S. Bethune, *Appl. Opt.* **20**, 1897 (1981).
 [15] L. D. Noordam, A. Ten Wolde and H. B. van Linden van den Heuvell, *Rev. Sci. Instrum.* **60**, 835 (1989).
 [16] L. D. Noordam, H. J. Bakker, M. P. de Boer, and H. B. van Linden van den Heuvell, *Opt. Lett.* **16**, 971 (1991).